UTAH GEOLOGICAL SURVEY
a division of
Utah Department of Natural Resources

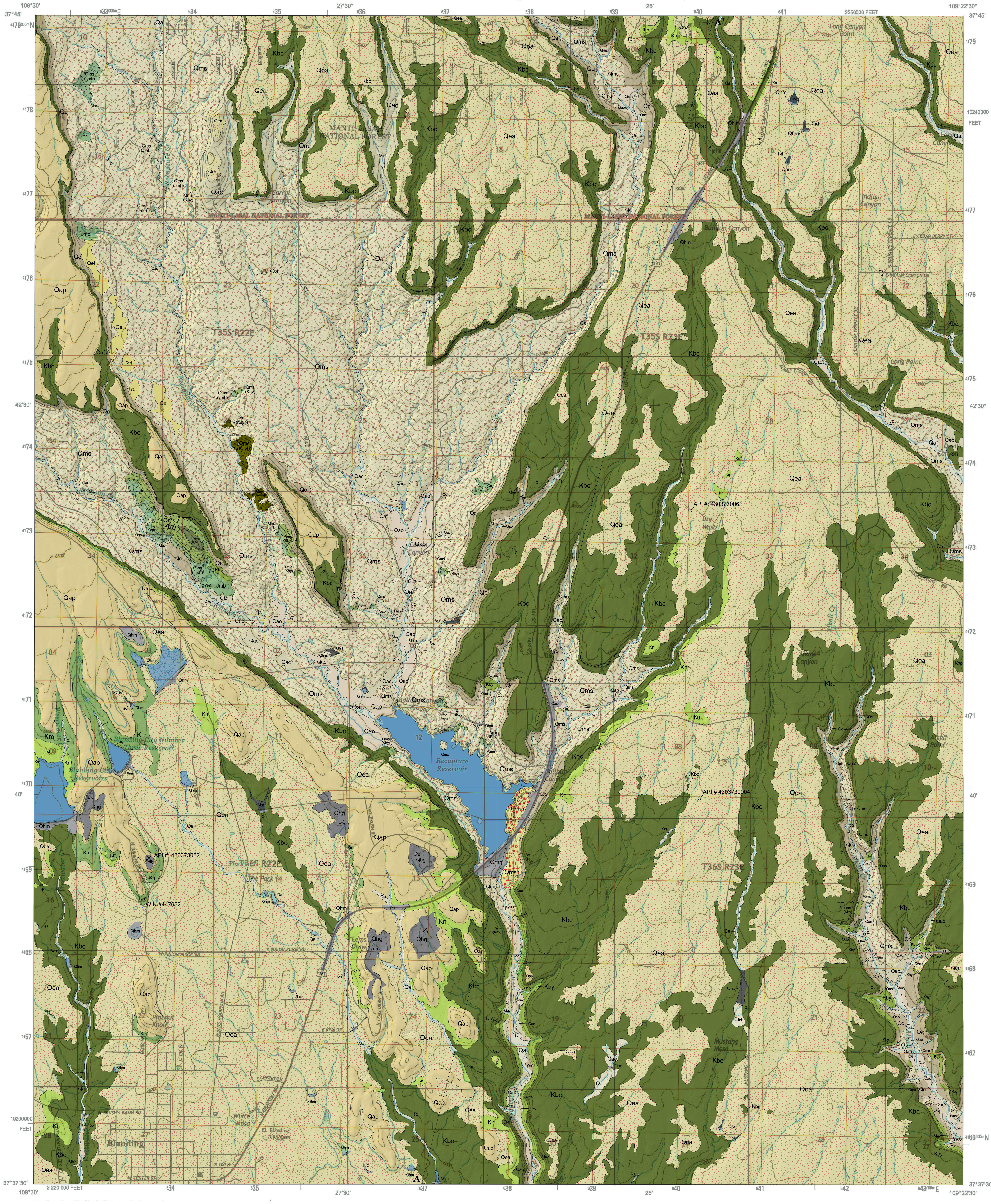

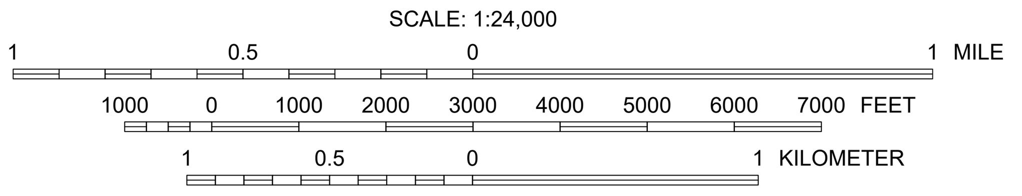

This open-file release makes information available to the public that has undergone only minimal peer review and may not conform to Utah Geological Survey technical, editorial, or policy standards. The map may be incomplete, and inconsistencies, errors, and omissions have not been resolved. The Utah Department of Natural Resources, Utah Geological Survey, makes no warranty, expressed or implied, regarding the suitability of this product for a particular use, and does not guarantee accuracy or completeness of the data. The Utah Department of Natural Resources, Utah Geological Survey, shall not be liable under any circumstances for any direct, indirect, special, incidental, or consequential damages with respect to claims by users of this product. For use at 1:24,000 scale.

This geologic map was funded by the Utah Geological Survey and the U.S. Geological Survey, National Cooperative Geologic Mapping Program, through USGS STATEMAP award number G23AC00466 (2023–2025). The views and conclusions contained in this document are those of the author and should not be interpreted as necessarily representing the official policies, either expressed or implied, of the U.S. Government.

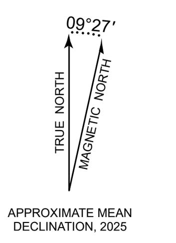

APPROXIMATE MEAN DECLINATION, 2025

Base from USGS US Topo Blanding North 7.5' Quadrangle (2014)
Hillshade from USGS National Map 3D Elevation Program (2025)
Projection and datum for base map and GIS data are UTM NAD83. The geology is accurately shown relative to cultural and topographic features on the US Topo base map.

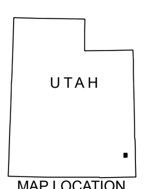

MAP LOCATION

Program Manager: Stefan M. Kirby
Project Manager: Stefan M. Kirby
GIS and Cartography: Austin J. Jensen
GIS and Cartography Reviews: Josh A. Dustin and Keilee A. Higgs
GeMS Reviews:Josh A. Dustin and Keilee A. Higgs

Utah Geological Survey
1594 West North Temple, Suite 3110
Salt Lake City, UT 84116-3154
(801) 537-3300
https://geology.utah.gov

https://doi.org/10.34191/OFR-771DM

INTERIM GEOLOGIC MAP OF THE BLANDING NORTH QUADRANGLE, SAN JUAN COUNTY, UTAH

by

Matthew C. Morriss

2025

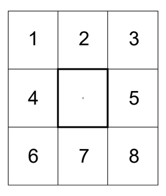

1. Mount Linnaeus
2. Abajo Peak
3. Monticello South
4. Mancos Jim Butte
5. Devil Mesa
6. Black Mesa Butte
7. Blanding South
8. Bradford Canyon

ADJOINING 7.5′ QUADRANGLE NAMES

LIST OF GEOLOGIC UNITS
(See booklet for complete unit description)

Qhm	Fill and disturbed land
Qhg	Gravel pits
Qhd	Dam impoundment sediments
Qa	Younger stream alluvium
Qao	Older stream alluvium
Qaf	Alluval-fan deposits
Qap	Pediment alluvium
Qc	Colluvial deposits
Qmsh	Historical landslide deposits
Qms	Landslide deposits
Qms (Kbc)	Landslide deposits involving the Burro Canyon Formation
Qms (Kby)	Landslide deposits involving the Yellow Cat Member of the Burro Canyon Formation
Qms (KJyb)	Landslide deposits involving the Yellow Cat Member of the Burro Canyon Formation & Brushy Basin Member of the Morrison Formation
Qms (Jmb)	Landslide deposits involving the Brushy Basin Member of the Morrison Formation
Qac	Mixed alluvium and colluvial
Qae	Mixed alluvium and eolian
Qea	Mixed eolian and alluvium
Qel	Eolian sand and loess deposits
Km	Mancos Shale
Kn	Naturita Formation
Kbc	Burro Canyon Formation
Kby	Burro Canyon Formation, Yellow Cat Member
Jmb	Morrison Formation, Brushy Basin Member
Jm	Morrison Formation, undivided (cross section only)
Jsr	San Rafael Group (cross section only)
Jn	Navajo Sandstone (cross section only)
Jk	Kayenta Formation (cross section only)
JŦw	Wingate Sandstone (cross section only)
Ŧc	Chinle Formation (cross section only)
Pc	Cutler Formation (cross section only)

GEOLOGIC SYMBOLS

- Contact – Dashed where approximately located
- Landslide scarp – Hachures on downdropped side
- 12 Strike and dip of inclined bedding
- 12 Strike and dip of inclined bedding, determined by 3-point problem on lidar data
- Sand and gravel pit
- Water well – Well Identification Number
- Drill hole, abandoned
- Drill hole, oil and gas well, abandoned
- A ______ A' Cross section line

CORRELATION OF MAP UNITS

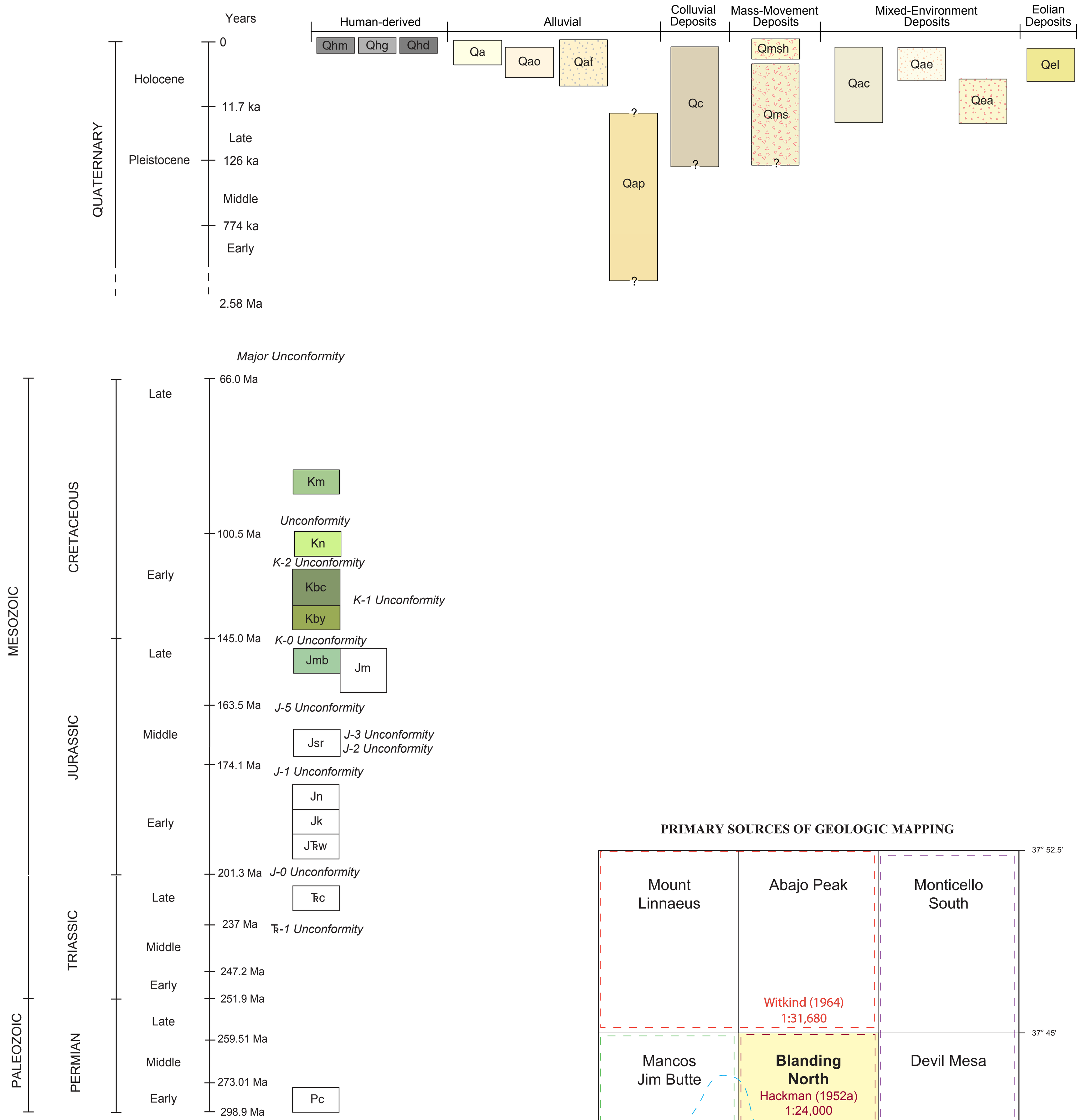

Timescale breaks from Walker and Geissman (2022)

LITHOLOGIC COLUMN

AGE		TECTONIC SETTING	DEPOSITIONAL ENVIRONMENT	GEOLOGIC UNIT		MAP SYMBOL	THICKNESS feet (meters)
QUATERNARY	Holocene	Exhumation and Colorado Plateau erosion	Alluvial and mass-wasting deposits in modern drainges and basins	Surficial deposits		Q Various	3–33 (1–10)
	Pleistocene		Alluvial and colluvial deposits draining periphery of Abajo Mountains	Oldest pediment alluvium		Qap	80–100 (24–30)
CRETACEOUS	Late	Marginal and deep water deposition in W. Interior Seaway	Shallow marine shales and mudstones	Mancos Shale		Km	<60 (< 18)
	Early		Marginal marine	Naturita Formation		Kn	30-40 (10–13)
		Foreland basin deposition proximal to elevated Mogollon Highlands to the south in Arizona	River channel and floodplain	Burro Canyon Formation		Kbc	120–300 (37–91)
			Lacustrine, fluvial, & interfluvial		Yellow Cat Member	Kby	~100 (33)
JURASSIC	Late	Distal foreland basin deposits of the Sevier fold-and-thrust belt	Floodplain and anastamosing rivers	Morrison Formation	Brushy Basin Member	Jmb	~515 (157)

LITHOLOGY/NOTES

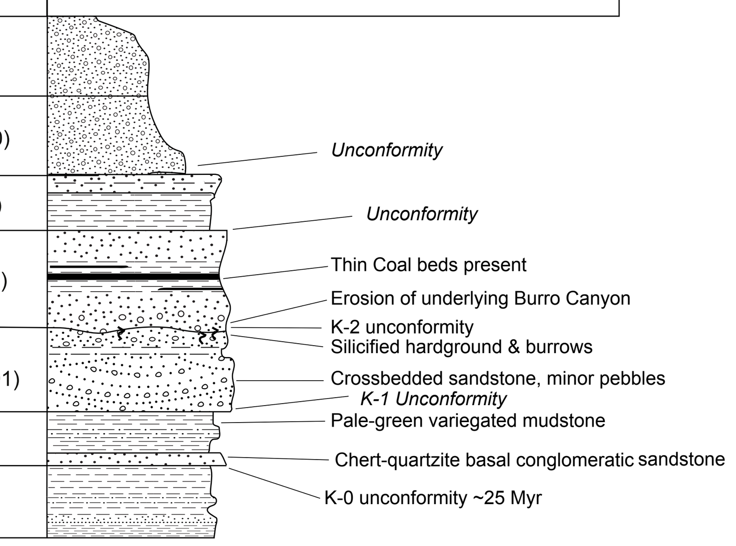

WELLS USED IN BLANDING NORTH QUDRANGLE MAPPING AND CROSS SECTION

ID	Well Information	WIN1/API2	Latitude (WGS 1984)	Longitude (WGS 1984)	Formation	Map Unit Symbol	Top* (feet)	Top (meters)	Thickness (feet)	Thickness (meters)	Comments
1	WTP Well	WIN 447652	37.6544	-109.4853	Mancos Shale	Km	0.5	0.2	0.5	0	
					Burro Canyon Formation	Kbc	5	1.5	265	81	
					Morrison	Jm	270	82	735	224	
					Entrada	Jsre	1005	306	180	55	
					Carmel	Jsrc	1185	361	145	44	
					Navajo	Jn	1130	344	550	168	
					Kayenta	Jk	1880	573	-	-	
2	Tenneco Blanding Unit 15-7	API 4303730892	37.659522	-109.484269	Morrison	Jm	295	90	918	280	
					Entrada	Jsre	1213	370	223	68	
					Carmel	Jsrc	-	-			Carmel Formation not picked
					Navajo	Jn	1436	438	545	166	
					Kayenta	Jk	1981	604	173	53	
					Wingate	Jw	2154	657	303	92	
					Chinle	Ŧrc	2457	749	999	304	
					Cutler	Pc	3456	1053	-	-	
3	Tenneco Bullpup Unit 1-8	API 4303730904	37.666482	-109.410501	Morrison	Jm	205	62	851	259	
					Entrada	Jsre	1056	322	217	66	
					Carmel	Jsrc		0			Carmel Formation not picked
					Navajo	Jn	1273	388	530	162	
					Kayenta	Jk	1803	550	130	40	
					Wingate	Jw	1933	589	334	102	
					Chinle	Ŧc	2267	691	1128	344	
					Cutler	Pc	3395	1035	-	-	
4	Utah State 1	API 4303730061	37.697105	-109.411674	Morrison	Jm	-				Morrison formation not picked
					Summerville	Jsrs	930	283	120	37	
					Entrada	Jsre	1050	320	140	43	
					Carmel	Jsrc	1190	363	85	26	
					Navajo	Jn	1275	389	425	130	
					Kayenta	Jk	1700	518	230	70	
					Wingate	Jw	1930	588	370	113	
					Chinle	Ŧc	2300	701	850	259	
					Cutler	Pc	3150	960	-	-	

* Formation tops picked by well drillers; 1) Well Identification Number; 2) American Petroleum Institute numbering
Well 1 data from Utah Division of Water Rights well database; Wells 2,3,4 data are from Utah Division for Oil, Gas, and Mining well database

PRIMARY SOURCES OF GEOLOGIC MAPPING

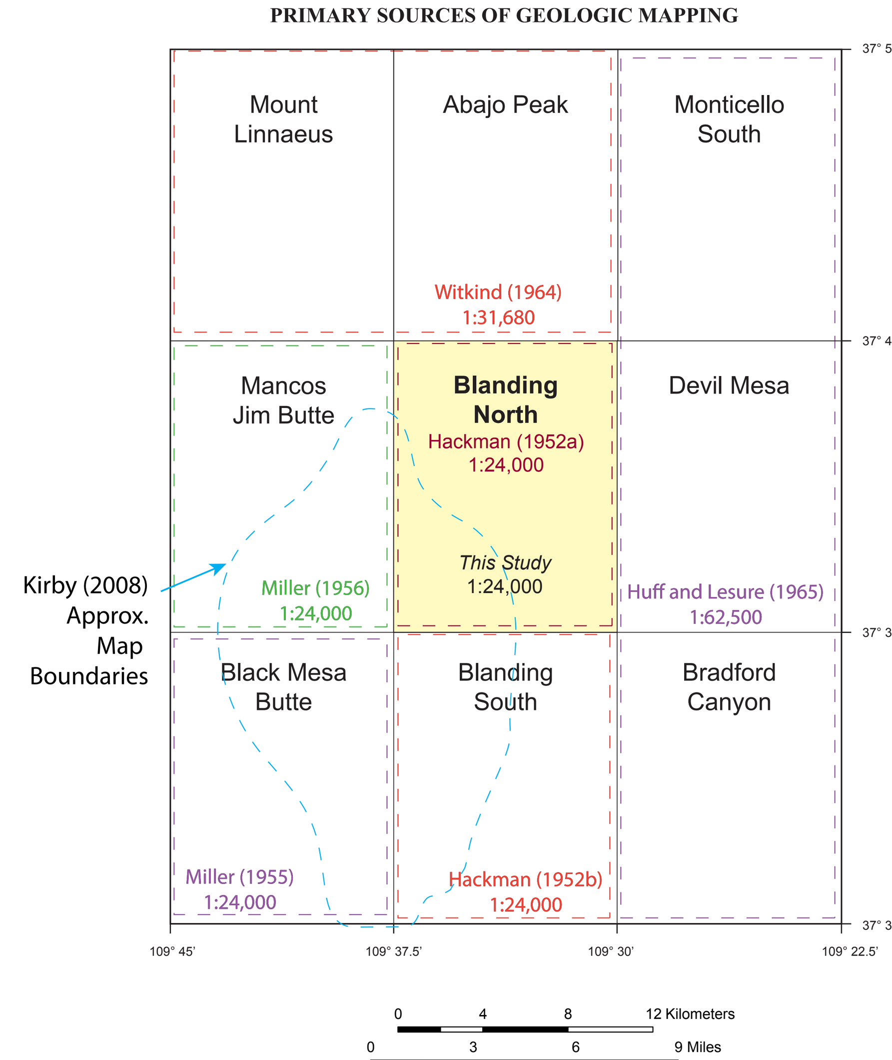

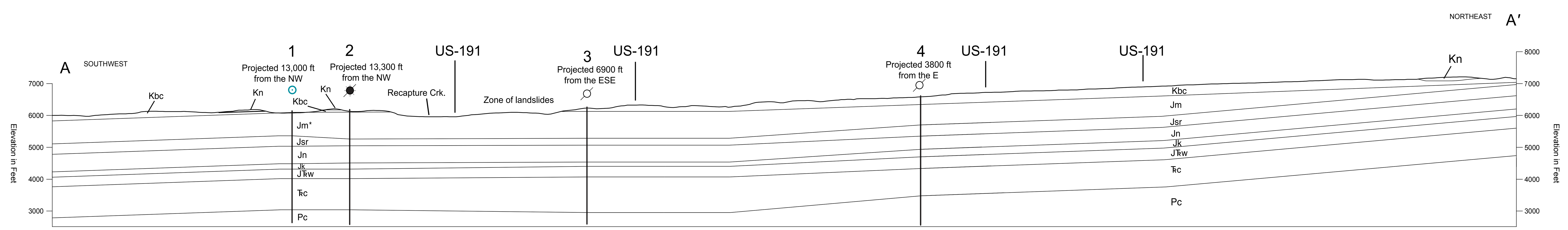

*Brushy Basin lumped with Morrison Formation (Jm), undivided in cross section. Quarternary units not shown.

INTERIM GEOLOGIC MAP OF THE BLANDING NORTH QUADRANGLE, SAN JUAN COUNTY, UTAH

by

Matthew C. Morriss

Suggested citation:

Morriss, M.C., 2025, Interim geologic map of the Blanding North quadrangle, San Juan County, Utah: Utah Geological Survey Open-File Report 771DM, 12 p., 2 plates, scale 1:24,000, https://doi.org/10.34191/OFR-771DM.

Disclaimer

This geologic map was funded by the Utah Geological Survey and the U.S. Geological Survey, National Cooperative Geologic Mapping Program, through USGS STATEMAP award number G23AC00466 (2023–2025). The views and conclusions contained in this document are those of the author and should not be interpreted as necessarily representing the official policies, either expressed or implied, of the U.S. Government.

OPEN-FILE REPORT 771DM
UTAH GEOLOGICAL SURVEY
UTAH DEPARTMENT OF NATURAL RESOURCES
2025

INTRODUCTION

The Blanding North 7.5′ quadrangle is near the southeastern corner of Utah, centered in San Juan County. The quadrangle is within the Colorado Plateau physiographic province and the Blanding Basin sub-province (Fenneman and Johnson, 1946), and is on the south flank of the Abajo Mountains. The Abajo Mountains are cored by an Oligocene suite of laccoliths coeval with other mountain ranges across the plateau including: the Henry, La Sal, and Navajo Mountains of Utah; the Ute and La Plata Mountains of Colorado; and the Carrizo Mountains of Arizona (Witkind, 1964). The Abajo intrusive rocks are not exposed in the Blanding North quadrangle, but the laccoliths of the Abajo Mountains provide the primary dips encountered across the map area, which are steeper to the north and gentler to the south (Witkind, 1964). The quadrangle ranges in elevation from 5695 ft (1736 meters [m]) to ~7450 ft (~2270 m) with the highest elevations in the northern part of the quadrangle, and lowest elevations in incised canyons in the southern margins of the map area.

U.S. Highway 191 bisects the quadrangle from north to south. The central part of the quadrangle includes Recapture Reservoir and dam along with the tributaries to the incised channels of Johnson and Recapture Creeks. Upgradient tributaries of these creeks include Bullpup Canyon, Bulldog Canyon, and Carrol Canyon. In the southwestern corner of the quadrangle is the city of Blanding, Utah. Blanding is the most populous city within San Juan County. Most of the land within the quadrangle is privately owned, supporting both dry land and irrigated farming operations and extensive water works of dams and smaller water and sediment retention structures. The next largest land holdings are Federal Lands, both Bureau of Land Management administered in the southern three-quarters of the quadrangle and U.S. Forest Service along the quadrangle's northern boundary. Small tracts owned by the Utah Schools and Institutional Trust Lands are scattered across the southern half of the quadrangle.

The primary goal of this mapping effort is to provide up-to-date geologic information on the geology surrounding the city of Blanding. This mapping effort is undertaken to better characterize the Mesozoic stratigraphy and units exposed in and around Blanding, as well as add context to surficial deposits and potential for geologic hazards in the region, namely landslides.

PREVIOUS WORK

This mapping effort builds on previous mapping presented in a 2008 study on groundwater in the area (Kirby, 2008) (see Index to Mapping Sources, Plate 2). This work involved geologic mapping at 1:50,000 scale across the southwestern quarter of the quadrangle. Kirby's (2008) map was the first to break out the Naturita and Burro Canyon Formations. Hackman, (1952a) and the coarse scale geologic mapping of the Cortez 1° x 2° sheet in southeastern Utah had lumped these units (Haynes et al., 1972). The Hackman (1952a) map was prepared in cooperation between the U.S. Geological Survey and Atomic Energy Commission and is part of this region's uranium exploration history. The new unit descriptions and stratigraphic division of the Naturita and Burro Canyon Formations utilized by Kirby (2008) were replicated in this Blanding North mapping.

METHODS

The author compiled and mapped the geology in the Blanding North quadrangle through a combination of GPS-enabled tablet (Apple iPad) with ESRI Field Maps © app and one-meter resolution light detection and ranging (lidar) data (U.S. Geological Survey, 2018, 2024). Through the mapping process, the previous geologic maps in the region (Hackman, 1952a; Kirby, 2008) were referenced for unit descriptions and some line work, but the author largely developed his own geologic line work across the quadrangle. Mapping was further aided by the help of relative elevation models, a derivative from a DEM to ascertain the elevation of different terrace treads above the modern river channel (Slaughter and Hubert, 2014; Larrieu, 2022). Satellite and aerial imagery were also used to aid in mapping. Google satellite-based imagery, and National Agriculture Imagery Program (NAIP) aerial imagery from 2018 were used. The final map was compiled in ESRI ArcGIS Pro and Adobe Illustrator was used to create and compile Plate 2 materials. Well location and formation top depth information was taken from oil and gas wells in the Utah Division of Oil, Gas and Mining database (Utah Division of Oil, Gas and Mining, 2025), and a water well from Burk et al. (2014). Modern geologic mapping on the periphery of the Blanding North quadrangle for edge matching of Blanding North is limited. However, the area was well covered by maps of varying quality from Kirby's (2008) field mapping to strictly aerial photograph-based mapping (e.g., Hackman, 1952). Adjoining work by Huff and Lesure (1965) mapped the Monticello South, Devil Mesa, and Bradford Canyon quadrangles at 1:62,500 scale. Witkind (1964) mapped the Mount Linnaeus and Abajo Peak quadrangles to the north and west of Blanding North at 1:31,680 scale. The Mancos Jim Butte to the west and Black Mesa Butte to the west and southwest were mapped from aerial photographs at 1:24,000 scale by Miller (1955, 1956). Both Blanding North and South were mapped from aerial photographs at 1:24,000 scale by Hackman (1952a, 1952b). These maps were used to a limited extent, and some edge matching work was done using Witkind (1964) and Huff and Lesure (1965).

GEOLOGY

Bedrock Stratigraphy

The bedrock stratigraphy in the quadrangle is a limited section of Mesozoic rocks that include the Morrison, Burro Canyon, Naturita, and Mancos Formations. The oldest exposed unit in the map area is the Late-Jurassic Brushy Basin Member of the Morrison Formation (see for more details Kirkland et al., 2020). The type locality for the Brushy Basin is 2.5 miles (~4 km) to the west of the Blanding North quadrangle in Brushy Basin Wash as described by Gregory (1938). The Brushy Basin Member of the Morrison has been dated via U-Pb dating on an ash at 150.67 ± 0.32 Ma (Kirkland et al., 2020), placing the Brush Basin in the Tithonian. The Morrison Formation was deposited in a variety of environments ranging from alluvial plains, riverine, and floodplain environments, stretching from central Utah to almost the New Mexico-Oklahoma border (Dodson et al., 1980; Kirkland et al., 2020). At the time of deposition, there were distant highlands to the west of the Morrison depositional centers including mountains of the North American Cordilleran orogenic system and the soon to develop Sevier orogeny (Yonkee and Weil, 2015; Surpless et al., 2023). Paleocurrent directions in the Morrison broadly indicate a northeast and east directed flow pattern during this time (Dickinson and Gehrels, 2008).

The Brushy Basin Member outcrops in parts of Recapture and Johnson Creeks in Bulldog, Carrol, and Bullpup Canyons. Exposures are often poor and obscured by landslides, and most large landslides in the quadrangle are underlain by the Brushy Basin. This member of the Morrison Formation was deposited as mostly muddy floodplains with some slower flowing meandering stream channels, containing occasional floodplain lakes (Currie, 1998; Dickinson and Gehrels, 2008). The Brushy Basin is unconformably overlain by the Early-Cretaceous Burro Canyon Formation and its locally mappable Yellow Cat Member. Between these units is the K-0 unconformity (Pipiringos and O'Sullivan, 1978), which may represent ~25 million years of time in this part of the Colorado Plateau locally (Pipiringos and O'Sullivan, 1978; Demko et al., 2004; Kirkland et al., 2016). However, further work is needed to better constrain the timing of the basal Cretaceous unconformity.

The Burro Canyon Formation only has one formalized member in this quadrangle—the lower part called the Yellow Cat Member. The remainder of the formation is undivided and overlies the Yellow Cat (Stokes and Pheonix, 1948; Kirkland et al., 2020). Where exposure is poor (most of the quadrangle), the Burro Canyon Formation is undivided. Given its stratigraphic position, above the Morrison and below the Naturita Formation, the Burro Canyon has been proposed to correlate with the Cedar Mountain Formation north of the Colorado River (for more details see Young, 1960). However, a direct stratigraphic and geologic correlation between the two formations and their individual members has not yet been fully developed (Tschudy et al., 1984; Miller, 2015). Recently, Cedar Mountain Formation member nomenclature (i.e., Yellow Cat) has been applied to the lowermost member of the Burro Canyon (Kirkland et al., 2020).

The depositional environment for the Burro Canyon Formation was an active fluvial system (Miller, 2015). Paleocurrent indicators show north-flowing rivers that were actively transporting sediment from the high Bisbee basin's rift shoulder known as the Mogollon highlands (Bilodeau, 1986; Miller, 2015). This source area is further supported by the limited detrital zircon work of Dickinson (2018).

The top of the Burro Canyon Formation is a paleosurface, representing the K-2 unconformity (Pipiringos and O'Sullivan, 1978). The overall time represented by this unconformity is poorly constrained due to lack of robust geochronology in the region. Extrapolating from the known age of the top of the Cedar Mountain Formation and the depositional age of the Naturita elsewhere, this unconformity could range from 2 to 5 myr and up to ~10 myr (Hunt et al., 2011; Kirkland et al., 2016).

The unit above the K-2 unconformity is the Naturita Formation, formerly mapped as Dakota Formation (Hackman, 1952a; Kirby, 2008; Carpenter, 2014). Regionally the Naturita contains well-sorted, fine-grained sandstone, carbonaceous shale beds, scattered coal beds, and mudstone (Huff and Lesure, 1965). The depositional environment for the Naturita is a complex combination of fluvial, marginal marine, paludal, and transgressive littoral deposits related to subsidence and transgression of the Cretaceous Interior Seaway (Huff and Lesure, 1965; Slattery et al., 2013). Above the Naturita is another unconformity, the time length of which is poorly constrained in southeastern Utah (Gregson and Chure, 2000; Sprinkel, 2024). The

Mancos Shale is the youngest bedrock unit in the quadrangle. The Mancos records the incursion of the Cretaceous Interior Seaway. The basal Mancos may correlate regionally with the Tununk Member (J.I. Kirkland, Utah Geological Survey, written communication, 2024).

An unconformity lies atop Mancos Shale separating the bedrock units in the quadrangle and younger Quaternary deposits shed off the Abajo Mountains. Much of the recent landscape development has been driven by changes in regional base level—the San Juan River and uplift of the Abajo Mountains. The igneous intrusions of the Abajos deflected the surrounding sedimentary strata, the dips of which increasingly steepen with proximity to the main instrusive body (Witkind, 1964). This intrusion-caused deformation of the strata is reflected across the Blanding quadrangle and the broader region. These intrusions crystallized at ~28 Ma (Murray et al., 2019). The Colorado Plateau region has seen significant erosion due to regional knickpoint migration from the Colorado River downstream and significant exhumation (Murray et al., 2019). Rates of incision along the San Juan River at Bluff, Utah, (due south of Blanding) are ~0.113 mm yr^{-1} during the last 1.2 Ma (Albonico, 2021). This incision rate has potentially accelerated over the last 5 myr. This signal of more rapid incision has yet to fully propagate into Blanding, with only Recapture Creek showing any significant recent incision.

Geologic Structure

The surface bedrock exposures across the Blanding quadrangle are devoid of map-scale faults and folds, which is not inconsistent with the structural nature of the Colorado Plateau physiographic province. Other than large contractional features of the Laramide orogeny, the Colorado Plateau is largely lacking major geologic structures (e.g., Jepson et al., 2025). In Blanding specifically, the stratigraphy is exposed in a broad steeply to gently, south-dipping panel bisected by the modern canyons. Previous geophysical well log interpretations by Burk et al. (2014) mapped two concealed faults, the Lems Draw and Park faults, that trend north-northwest across the southern part of the Blanding North quadrangle. Based on the geophysical work, these faults are presumed to have throws on the order of 100 feet. No mapping conducted as part of this project saw any surface expression of nor stratigraphic offsets to indicate these faults exist. If present, these structures may predate the deposition of units overlying the Brushy Basin Member of the Morrison Formation.

Geologic Hazards

The most prominent geologic hazard in the Blanding North quadrangle are landslides. A significant part (~35%) of the quadrangle is mapped as some form of mass movement deposit. The exact timing of these failures is largely unclear, but based on their topographic expression and roughness some of these landslides have been recently active, and the potential for future mass wasting remains. A single historically active landslide is mapped along U.S. Highway 191 between mile marker 55 and 56 where the Utah Department of Transportation has had to repair the road multiple times, indicating modern movement.

There are no recorded major earthquake epicenters within the Blanding North quadrangle, nor are there any recorded major earthquakes near the quadrangle with clear geologic hazard implications (Bowman and Arabasz, 2017). There are also no records of historical flooding. The extensive construction of homes, businesses, and infrastructure on the Mancos Shale, and shale within the Naturita, Burro Canyon, and Morrison Formations may have the potential for exposure to expansive soils. Landslides could also affect the infrastructure in and around the Blanding North quadrangle.

DESCRIPTION OF MAP UNITS

QUATERNARY-TERTIARY SURFICIAL DEPOSITS

Human-Derived Deposits

Qhm **Fill and disturbed land** (historical) – Undifferentiated artificial fill and disturbed land related to construction, road embankments, and dam abutments; the extent of fill and disturbed land are based on the 2020 and 2022 1-meter lidar; this unit is only mapped in larger areas; unmapped fill is present within developed areas in and around the community of Blanding; thickness ~0 to 30 ft (0–10 m).

Qhg **Gravel pits** (historical) – Gravel pits and borrow pits; consists of active cuts and minor locally sourced fill; mostly developed in unit Qap; thickness ~0 to 30 ft (0–10 m).

Qhd **Dam impoundment sediments** (historical) –Backfill sediments from damming of perennial and ephemeral channels for water storage; largely silt dominated with some sand and minor gravel, thickness 0 to 25 ft (0–8 m).

Alluvial Deposits

Qa **Younger stream alluvium** (Holocene) – Light-brown to brownish-red; moderately sorted, unconsolidated sand and silt with minor clay and gravel; deposited by flood overbank, channel migration, and other active channel processes; forms modern channels and flood plains of Westwater Creek, Johnson Creek, Recapture Creek, and other drainages in the quadrangle; locally grades into alluvial-colluvial deposits (Qac) and is incised into older alluvial deposits (Qao); estimated thickness 3 to 33 ft (1–10 m).

Qao **Older stream alluvium** (Holocene) – Light-brown to reddish-brown; poorly to moderately sorted, unconsolidated silt, sand, and gravel; deposited by flood overbank, channel migration, and other active channel processes; forms terraces approximately 3 to 7 ft (1–2 m) above modern floodplains along Johnson Creek, Recapture Creek, and their tributaries; locally may grade into alluvial-colluvial deposits (Qac), but stratigraphic relationships remain uncertain; estimated thickness 3 to 33 ft (1–10 m).

Qaf **Alluvial-fan deposits** (Holocene? to Late Pleistocene) Light brown to reddish-brown; poorly to moderately sorted, angular to subangular, pebble to boulder clasts in a matrix of silt, sand, and minor clay; crudely stratified to massive; clast composition reflects local source areas; deposited by debris flows, debris floods, and channel processes at the mouths of active drainages; locally grades into younger stream deposits (Qa), older stream deposits (Qao), and alluvial-colluvial deposits (Qac); thickness 0 to 30 ft (0–9 m).

Qap **Pediment alluvium** (Pleistocene) – Brown to gray-brown; moderately to moderately well sorted, matrix-supported cobbles to small boulders; clasts predominantly sub-rounded to well-rounded, composed of green to brown to gray quartz diorite porphyry with white plagioclase and black hornblende phenocrysts; likely sourced from the Abajo Mountains to the north, some minor component of limestone and sandstone clasts potentially sourced from Paleozoic units in the Abajo Mountains; matrix consists of quartz-rich sand and carbonate-rich soil; characterized by poorly developed blocky ped structure and discontinuous sandy beds (sampled for optically stimulated luminescence dating in 2024, as of 04-18-2025 results are still pending); pedogenic carbonate forms root casts and coats entirely around and between clasts; contains multiple calcic soil horizons with Stage 3 carbonate development (Zamanian et al., 2016); locally overlies white to yellowish-white, semi-fissile shale beds of the Mancos Shale, sandstone of the Naturita Formation, and sandstone and conglomerate of the Burro Canyon Formation; consists of alluvial surfaces approximately 300 to 500 ft (90–150 m) above Johnson and Recapture Creeks; thickness 80 to 100 ft (24–30 m).

Colluvial Deposits

Qc **Colluvial deposits** (Holocene to Late Pleistocene?) – Poorly to moderately sorted, clay- to boulder-size, locally derived sediment deposited by slope wash and soil creep; commonly clast supported with a matrix of sand, silt, and clay; clasts commonly angular to subangular and very poorly sorted; composed primarily of sandstone, conglomerate, mudstone, and claystone clasts derived from the Burro Canyon Formation; found mostly along steep cliffs incised by regional drainages in the map area; deposited on moderate slopes and in shallow depressions directly below areas of steep slopes; may include small landslides, rockfalls, and debris flows that are too small to map separately; much of the bedrock in the map area is covered by a thin veneer of colluvium, but only the larger, thicker deposits with significant thickness and extent are mapped; mapped as small cones and debris aprons below cliff-forming units; thickness typically less than 30 feet (9 m), commonly between 3 and 15 feet (1–5 m).

Mass-Movement Deposits

Qmsh **Historical landslide deposits** (Historical to Late Pleistocene?) – Red, brown, green, and yellow to yellowish-green, and in places blueish-yellow; poorly sorted, clay- to boulder-size material with large rotational bedrock blocks; composed of boulders from the Burro Canyon Formation and sandstone and mudstone from the Yellow Cat Member of the Burro Canyon Formation and Brushy Basin Member of the Morrison Formation; characterized by chaotic bedding in displaced blocks and hummocky surface morphology; mapped along U.S. Highway 191 bracketing Recapture Reservoir dam; road displays active surface cracking and requires frequent resurfacing by the Utah Department of Transportation; detailed geotechnical investigations needed to determine age and stability; thickness 65 to 132 ft (20–40 m).

Qms **Landslide deposits** (Holocene to Late Pleistocene) – Red, brown, green, and yellow to yellow-green, and in places blueish-yellow; poorly sorted clay- to boulder-size material with large rotational bedrock blocks; composed of conglomeratic boulders from the Burro Canyon Formation and sandstone and shale from the Yellow Cat Member of the Burro Canyon Formation and Brushy Basin Member of the Morrison Formation; primarily characterized by chaotic bedding in displaced blocks and hummocky surface texture; makes up significant portions (~35%) of the Blanding North quadrangle in areas where drainages have incised through the Burro Canyon Formation sandstone and conglomerate beds to the softer Yellow Cat Member and Brushy Basin Member of the Morrison Formation; in places landslides are draped with eolian sand and loess; even landslides with subdued morphology (suggesting that they are older, weathered, and have not moved recently) may continue to exhibit slow creep or are capable of renewed movement if stability thresholds are exceeded (Ashland, 2003); age and stability determinations require detailed geotechnical investigations; many small or thin landslides may be present throughout the quadrangle but not mapped due to map scale; thickness 65 to 130 ft (20–40 m).

Qms (Kbc)

Landslide deposits involving the Burro Canyon Formation (Holocene to Late Pleistocene) – Red, brown, and tan- yellow; poorly sorted clay- to boulder-size material with large rotational bedrock blocks; composed of conglomeratic boulders and sandstone blocks from the Burro Canyon Formation; sandstone components are typically white to variegated, medium- to coarse-grained, well-rounded quartz sandstone, commonly unbedded with locally developed cross-beds and foresets; conglomerate clasts include matrix-supported, well-rounded chert and limestone clasts up to 3 ft (1 m) thick; interbedded green to blue shale, mudstone, and claystone fragments also present; displaced blocks may exhibit bioturbation including burrows and possible root casts, case hardening, and silicified hardgrounds; primarily characterized by chaotic bedding in displaced blocks and hummocky surface texture; makes up significant portions (~35%) of areas where drainages have incised through the Burro Canyon Formation sandstone and conglomerate beds; in places landslides are draped with eolian sand and loess; even landslides with subdued morphology (suggesting they are older, weathered, and have not moved recently) may continue to exhibit slow creep or are capable of renewed movement if stability thresholds are exceeded (Ashland, 2003); age and stability determinations require detailed geotechnical investigations; thickness 65 to 130 ft (20–40 m).

Qms (Kby)

Landslide deposits involving the Yellow Cat Member of the Burro Canyon Formation (Holocene to Late Pleistocene) – Pale green to variegated chaotic, poorly sorted clay and sandy debris; in places, intact mudstone and claystone with distinctive dark-red to reddish-brown ferruginous paleosol where original bedding is visible; in places landslides are draped with eolian sand and loess; even landslides with subdued morphology (suggesting that they are older, weathered, and have not moved recently) may continue to exhibit slow creep or are capable of renewed movement if stability thresholds are exceeded (Ashland, 2003); age and stability determinations require detailed geotechnical investigations; many small or thin landslides may be present throughout the quadrangle but not mapped due to map scale; overall very poor exposure, but unit is best exposed on north side of Johnson Creek upstream from Recapture Reservoir; thickness 65 to 130 ft (20–40 m).

Qms (KJyb)

Landslide deposits involving the Yellow Cat Member of the Burro Canyon Formation and the Brushy Basin Member of the Morrison Formation (Holocene to Late Pleistocene) – Variegated chaotic deposit with poorly sorted clay and sandy debris; colors range from pale green to red, purple, and white; consists of disturbed mudstone, claystone, and shale, with distinctive dark-red to reddish-brown ferruginous paleosol where original bedding is preserved; minor interbedded sandstone present, typically medium- to coarse-grained, lenticular, and laterally discontinuous; age and stability determinations require detailed geotechnical investigations; many small or thin landslides may be present throughout the quadrangle but not mapped due to map scale; overall very poor exposure, but unit is best exposed on north side of Recapture Creek upstream from Recapture Reservoir; thickness 65 to 130 ft (20–40 m).

Qms (Jmb)

Landslide deposits involving the Brushy Basin Member of the Morrison Formation (Holocene to Late Pleistocene) – Variegated red, green, purple, and white; chaotic mudstone, claystone, and shale with minor interbedded sandstone; sandstone beds are medium to coarse grained, lenticular, laterally discontinuous where bedding is preserved and visible; in places landslides are draped with eolian sand and loess; even landslides with subdued morphology (suggesting that they are older, weathered, and have not moved recently) may continue to exhibit slow creep or are capable of renewed movement if stability thresholds are exceeded (Ashland, 2003); age and stability determinations require detailed geotechnical investigations; many small or thin landslides may be present throughout the quadrangle but not mapped due to map scale; overall very poor exposure, but unit is best exposed on north side of Johnson Creek upstream from Recapture Reservoir; thickness 65 to 130 ft (20–40 m).

Mixed-Environment Deposits

Qac **Mixed alluvium and colluvial deposits** (Holocene to Late Pleistocene) – Brown to reddish-brown; poorly to moderately sorted, generally poorly stratified sediment ranging from clay to boulder size; clasts rounded to angular; consists of intermixed alluvial and colluvial deposits that grade into one another and cannot be differentiated at map scale; mapped at the base of steep slopes in incised canyons of the quadrangle where deposits are predominantly fan alluvium, and in small drainages where stream alluvium, fan alluvium, and colluvium are intermixed; small, unmapped deposits likely present in most minor drainages; areas of Qac have potential for debris-flow and flood hazards; thickness less than 15 ft (5 m).

Qae **Mixed alluvium and eolian deposits** (Holocene to Late Pleistocene) – Brown to light-brown, and red; moderately to well-sorted, unconsolidated mud, silt, and sand deposited by both alluvial and eolian processes; consists of alluvial deposits reworked by wind and intermixed with windblown sand and silt; mapped southeast of Recapture Reservoir dam where alluvial channels have been inundated by windblown sand and silt; thickness 3 to 40 ft (1–12 m).

Qea **Mixed eolian and alluvium deposits** (Holocene to Late Pleistocene) – Light-brown to brown to red; moderately to well-sorted, unconsolidated sand and silt with minor gravel; predominantly deposited by eolian processes with subordinate alluvial and debris-flow deposits; unit caps the majority of the mesa tops in the quadrangle; thickness 3 to 20 ft (1–6 m).

Qel **Eolian sand and loess deposits** (Holocene to Late Pleistocene) – Light-brown to tan; well-sorted, unconsolidated sand and silt; deposited by eolian processes; unit found in lee side of landslide scarps above Recapture Creek; thickness 3 to 10 ft (1–3 m).

BEDROCK UNITS

Major unconformity

CRETACEOUS

Km **Mancos Shale** (Late Cretaceous, Cenomanian) – White to light-gray to dark gray-green; thinly bedded to fissile marine shale with distinctive yellowish-white splotchy weathering pattern; contains thin—less than 2 ft (0.7 m)—interbeds of sandstone and siltstone; pelecypod fossils common throughout (Huff and Lesure, 1965; Haynes et al., 1972; Kirby, 2008); typically poorly exposed, forms slopes; commonly preserved beneath Qap deposits; deposited during transgression and highstand of the Cretaceous Western Interior Seaway; the basal Mancos in the quadrangle may correlate with the Tununk Member of the Mancos Shale (Elder and Kirkland, 1994; Kirkland et al., 2016; J.I. Kirkland, written communication, 2024); thickness variable, typically less than 60 ft (18 m).

Unconformity

Kn **Naturita Formation** (Early Cretaceous, Cenomanian?) – Yellow to yellow-brown; fine- to medium-grained, quartzose sandstone with distinctive red staining and iron oxide splotches; contains bioturbation and carbonized wood casts; sand is moderately well rounded with occasional angular chert clasts; near its base the unit locally includes rip-up clasts of underlying Burro Canyon Formation (Kirby, 2008); sedimentary structures include climbing ripples, poorly developed foresets, trough and planar cross-bedding, with sandstone beds up to 20 ft (6 m) thick in lower part; interbedded with coal, carbonaceous shales, green to gray-blue mudstones, and organic-rich layers; the upper part characterized by carbonaceous mudstone, siltstone, and sandstone beds less than 10 ft (3 m) thick (Huff and Lesure, 1965; Gloyn et al., 1995); forms relatively nondescript outcrops with distinctive brownish-red soils, small slopes, and "slickrock" sandstone benches (Kirby, 2008); sandstone bodies commonly interfinger or pinch out into mudstone or shale within several hundred feet; lower contact erosional with underlying Burro Canyon Formation; small poorly exposed Naturita outcrops are included in the Burro Canyon Formation on Plate 1; the Naturita is locally absent and the Mancos may rest directly on the Burro Canyon Formation; this unit has previously been mapped as "Dakota Formation" in this region and is still named as such in Colorado (Carpenter, 2014); thickness approximately 30 to 40 ft (10–13 m).

K-2 Unconformity

Kbc **Burro Canyon Formation** (Early Cretaceous, early Albian to Barremian) – White to variegated; medium- to coarse-grained, well-rounded quartz sandstone and conglomerate with interbedded green to blue shale, mudstone, claystone; sandstone is commonly unbedded with locally developed cross-beds and foresets, forms prominent cliffs 40 to 60 ft (12–18 m) high, locally up to 80 to 100 ft (24–31 m) along mesa margins (Montgomery, 1980); conglomerate beds up to 3 ft (1 m) thick are matrix-supported and composed of well-rounded chert and limestone clasts; individual channel deposits commonly display scouring into underlying sandstone and fining-upward sequences; sandstone exhibits laminar flow structures and variegated weathering colors though typically white on fresh surfaces; upper most sandstone shows extensive bioturbation including burrows and possible tree casts, distinctive case hardening, and silicified hardgrounds particularly near upper contact; this may be a paleosurface atop the Burro Canyon Formation; cross-bedded channel sandstones and laterally discontinuous blue to green claystone interbeds dominate the lower part; while mudstone, claystone, and interbedded fines dominate over sandstone in upper parts (Craig, 1981); deposited under fluvial conditions associated with the Mogollon Highlands to the south (Miller, 2015); in places, this main body of the Burro Canyon may cut down through underlying Yellow Cat Member, leaving no remaining Yellow Cat; mapped Burro Canyon Formation locally includes Naturita Formation in areas of poor exposure near Qea contacts; Early Cretaceous age based on palynomorphs from the top of the formation north of the map area and fission track dating on detrital zircons with an age of 125 ± 10 Ma (Craig, 1981; Tschudy et al., 1984); lower contact is sharp and represents the K-1 unconformity with underlying Yellow Cat Member; thickness approximately 120 to 300 ft (37–85 m).

K-1 Unconformity

Kby **Burro Canyon Formation, Yellow Cat Member** (Early Cretaceous) - Pale green to variegated mudstone and claystone with distinctive dark-red to reddish-brown ferruginous paleosols; basal part is gray to light-colored sandstone and conglomerate containing chert and quartzite pebbles; mudstones weather to flat or concave slopes rather than convex profiles with a popcorn surface texture, suggesting the presence of smectite or shrink-swell clays; contains dark-green claystones with plant fragments in upper part; beds are locally mottled where preserved immediately below K-1 unconformity; locally mapped as the unit that is the lower part of the Burro Canyon Formation; upper contact is sharp and erosional with overlying fluvial sandstones of main body of Burro Canyon Formation; age is Early Cretaceous based on stratigraphic position above K-0 unconformity (Kirkland et al., 2020); member nomenclature follows Kirkland et al. (2020); thickness is approximately 100 ft (30 m).

K-0 Unconformity

JURASSIC

Jmb **Morrison Formation, Brushy Basin Member** (Late Jurassic) – Variegated red, green, purple, and white mudstone, claystone, and shale with minor thin interbedded sandstone; sandstone beds are medium to coarse grained, lenticular, laterally discontinuous; lower Brushy Basin contains higher proportion of sand-sized material with beds of sandstone, muddy sandstone, and smectitic sandy mudstone; middle to upper parts dominated by smectitic clays that display characteristic "popcorn" weathering; deposited in mixed lacustrine and fluvial environments; forms poorly exposed slopes with characteristic convex weathering profile commonly mantled by landslide complexes and vegetation; upper contact is disconformable with mudstones of the basal Yellow Cat Member of the Burro Canyon Formation; age is 150.67 ± 0.32 Ma based on U-Pb dating of zircons from volcanic ash near top of unit (Kirkland et al., 2020); thickness approximately 515 ft (157 m) thinning to the north, but the base of the unit is not exposed in the map area.

SUBSURFACE BEDROCK UNITS

JURASSIC

Jm **Morrison Formation, undivided** (Late Jurassic, Kimmeridgian to Oxfordian) – Shown only in cross section; complex sequence of variegated mudstone, sandstone, and minor limestone consisting of four main members (descending): Brushy Basin Member composed of variegated smectitic mudstone with minor sandstone lenses; Westwater Canyon Member composed of lenticular, white to greenish-yellow sandstone with red shale partings; Recapture Member composed of reddish-brown mudstone and sandstone; and Salt Wash Member composed of white conglomeratic sandstone interbedded with red mudstone; deposited in fluvial, lacustrine, and floodplain environments (Turner and Peterson, 2004; Doelling, 2006; Kjemperud et al., 2008; Kirkland et al., 2020); preserved thickness varies but generally 250 to 850 ft (76–260 m) thick (Kirkland et al., 2020).

J-5 Unconformity

Jsr **San Rafael Group** (Late to Middle Jurassic) – Shown only in cross section; reddish-brown to yellowish-gray interbedded sandstone, siltstone, and mudstone sequence; upper **Summerville Formation** consists of thin-bedded reddish-brown to greenish-gray sandstone, siltstone, and mudstone with local gypsum veinlets; middle part **Entrada Sandstone** includes pale-reddish-brown to yellowish-brown, fine- to medium-grained, massive cross-bedded sandstone that commonly weathers to rounded "slickrock" surfaces; lower **Carmel Formation** characterized by pale yellowish-gray to brownish-gray, calcareous, fine- to medium-grained sandstone interbedded with reddish-brown to greenish-gray mudstone and siltstone; deposited in coastal environments ranging from eolian dune fields to marginal-marine and sabkha settings; contains the J-2 and J-3 unconformities (Doelling, 2006; Doelling et al., 2013; Lucas, 2014); combined thickness approximately 230 to 340 ft (70–103 m) (Doelling, 2006; Doelling et al., 2013; Lucas, 2014).

J-1 Unconformity

Jn **Navajo Sandstone** (Early Jurassic) – Shown only in cross section; pale-yellowish-gray to moderate-reddish-brown, fine- to medium-grained, massive sandstone; well-sorted, rounded to subrounded, frosted quartz grains in prominent cross-bed sets up to 60 ft (20 m) thick; rare thin lenses of gray carbonate and siltstone; deposited primarily in large sand desert (erg) environment (Pipiringos and O'Sullivan, 1978; Doelling, 2006; Doelling et al., 2013); approximately 390 to 550 ft (119–167 m) thick (Pipiringos and O'Sullivan, 1978; Doelling, 2006; Doelling et al., 2013).

Jk **Kayenta Formation** (Early Jurassic) – Shown only in cross section; pale-reddish-brown to purplish-red, lenticular, medium- to thick-bedded sandstone and silty sandstone with interbedded reddish-brown siltstone and mudstone; contains planar- to cross-bedded intervals and sparse limestone lenses; deposited in fluvial-lacustrine environment with eolian influence (Doelling, 2006, p. 200); 143 to 213 ft (44–65 m) thick (Pipiringos and O'Sullivan, 1978; Doelling, 2006; Doelling et al., 2013).

JURASSIC-TRIASSIC

JŦw **Wingate Sandstone** (Early Jurassic to Late Triassic) – Shown only in cross section; pale- to moderate-reddish-orange, massive, cross-bedded, very fine to fine-grained sandstone; well-sorted, subangular to subrounded, frosted grains; typically forms massive cliff commonly marked by desert varnish and vertical joints; deposited in eolian environment (Clemmensen et al., 1989; Doelling, 2006); 335 to 372 ft (102–113 m) thick (Clemmensen et al., 1989; Doelling, 2006).

J-0 Unconformity

TRIASSIC

Ŧc **Chinle Formation** (Late Triassic) –Shown only in cross section; complex intertonguing sequence of volcaniclastic-bearing fluvial and lacustrine deposits including sandstone, conglomerate, mudstone, siltstone, claystone, and minor limestone; consists of up to six members (descending order): Church Rock, Owl Rock, Petrified Forest, Moss Back, Monitor Butte, and Shinarump Members; deposited in fluvial-lacustrine environment of northwest-flowing trunk river system (Repenning et al., 1969; Doelling, 2006; Rasmussen et al., 2021); major regional unconformity at base; 870 to 1100 ft (265–335 m) thick (Repenning et al., 1969; Doelling, 2006; Rasmussen et al., 2021).

₮-1 *Unconformity*

PERMIAN

Pc **Cutler Group** (Early Permian) – Shown only in cross section; complex sequence of intertonguing formations including: upper **Organ Rock Shale** consisting of dark-reddish-brown to grayish-red micaceous siltstone and fine- to medium-grained sandstone (166 to 309 ft [51–94 m] thick); middle **Cedar Mesa Sandstone** consisting of light-grayish-orange, cross-bedded, fine-grained sandstone with reddish-brown to grayish-green siltstone lenses (1000 to 1200 ft [300–360 m] thick); and basal **Halgaito Formation** deposited in environments ranging from eolian to fluvial, tidal-flat, and marginal marine settings during final stage of Paradox basin development (Doelling et al., 2013); minimum thickness approximately 1200 to 1500 ft (365–460 m) (Doelling et al., 2013; Hintze and Kowallis, 2021; Willis and Higgs, 2024); total thickness 2370 to 3000 ft (720-915 m).

ACKNOWLEDGMENTS

The Blanding North quadrangle was mapped as part of the U.S. Geological Survey STATEMAP award # G23AC00466. I thank James Kirkland of the UGS for discussions concerning the geology of the quadrangle. UGS staff, including Stefan Kirby, Donald Clark, Stephanie Carney, Lucy Jordan, and Darlene Batatian, provided important reviews of this map. Thanks to Austin Jensen of the UGS for helping with GIS, cartography, and construction of all plates and figures. Subigya Shah and Josh Dustin of the UGS provided a review of the GIS and cartography.

REFERENCES

Albonico, M.T., 2021, The birth and incision history of the San Juan River in the past 5 Ma: Albuquerque, University of New Mexico, M.S. thesis, 83 p.

Ashland, F.X., 2003, Characteristics, causes, and implications of the 1998 Wasatch Front landslides, Utah: Utah Geological Survey Special Study SS-105, https://doi.org/10.34191/SS-105.

Bilodeau, W.L., 1986, The Mesozoic Mogollon Highlands, Arizona: An Early Cretaceous rift shoulder: The Journal of Geology, v. 94, no. 5, p. 724–735, https://doi.org/10.1086/629077.

Bowman, S.D., and Arabasz, W.J., 2017, Utah earthquakes (1850–2016) and Quaternary faults: Utah Geological Survey Map M-277, scale 1:500,000, https://doi.org/10.34191/M-277.

Burk, N.I., Loughlin, W.D., and Conway, C.M., 2014, Investigation and successful development of the Navajo Sandstone aquifer near blanding, Utah, *in* Maclean, J.S., Biek, R.F., and Huntoon, J.E., editors, Geology of Utah's far south: Utah Geological Association Publication 43, p. 135–152.

Carpenter, K., 2014, Where the sea meets the land—The unresolved Dakota problem in Utah, *in* Maclean, J.S., Biek, R.F., and Huntoon, J.E., editors, Geology of Utah's Far South: Utah Geological Association UGA Publication 43, p. 357–372.

Clemmensen, L.B., Olsen, H., and Blakey, R.C., 1989, Erg-margin deposits in the Lower Jurassic Moenave Formation and Wingate Sandstone, southern Utah: Geological Society of America Bulletin, v. 101, no. 6, p. 759–773, https://doi.org/10.1130/0016-7606(1989)101%3C0759:EMDITL%3E2.3.CO;2.

Craig, L.C., 1981, Lower Cretaceous rocks, southwestern Colorado and southeastern Utah, in Wiegland, D.L., editor, Geology of the Paradox Basin: Denver, Colorado, Rocky Mountain Association of Geologists Field Conference, p. 195–200.

Currie, B.S., 1998, Upper Jurassic-Lower Cretaceous Morrison and Cedar Mountain Formations, NE Utah-NW Colorado—Relationships between nonmarine deposition and early Cordilleran foreland-basin development: SEPM Journal of Sedimentary Research, v. 68, no. 4, p. 632–652, https://doi.org/10.1306/D426882E-2B26-11D7-8648000102C1865D.

Demko, T.M., Currie, B.S., and Nicoll, K.A., 2004, Regional paleoclimatic and stratigraphic implications of paleosols and fluvial/overbank architecture in the Morrison Formation (Upper Jurassic), Western Interior, USA: Sedimentary Geology, v. 167, no. 3–4, p. 115–135, https://doi.org/10.1016/j.sedgeo.2004.01.003.

Dickinson, W.R., 2018, Tectonosedimentary relations of Pennsylvanian to Jurassic strata on the Colorado Plateau: Geological Society of America Special Paper 533, 184 p., https://doi.org/10.1130/2018.2533.

Dickinson, W.R., and Gehrels, G.E., 2008, Sediment delivery to the Cordilleran foreland basin—Insights from U-Pb ages of detrital zircons in Upper Jurassic and Cretaceous strata of the Colorado Plateau: American Journal of Science, v. 308, no. 1, p. 1–48, https://doi.org/10.2475/01.2008.01.

Dodson, P., Behrensmeyer, A.K., Bakker, R.T., and McIntosh, J.S., 1980, Taphonomy and paleoecology of the dinosaur beds of the Jurassic Morrison Formation: Paleobiology, v. 6, no. 2, p. 208–232., https://doi.org/10.1017/S009483730000676X.

Doelling, H.H., 2006, Geologic map of the La Sal 30′ x 60′ quadrangle, San Juan, Wayne, and Garfield Counties, Utah, and Montrose and San Miguel Counties, Colorado: Utah Geological Survey Map M-205DM, scale 1:100,000, https://doi.org/10.34191/M-205DM.

Doelling, H.H., Sprinkel, D.A., Kowallis, B.J., and Kuehne, P., 2013, Temple Cap and Carmel Formations in the Henry Mountains basin, Wayne and Garfield Counties, Utah, *in* Morris, T.H., and Ressetar, R., editors, The San Rafael Swell and Henry Mountains Basin—Geologic centerpiece of Utah: Utah Geological Association Publication 42, p. 279–318.

Elder, W.P., and Kirkland, J.I., 1994, Cretaceous paleogeography of the southern Western Interior region, in Caputo, M.V., Peterson, J.A., and Franczyk, K.J., editors, Mesozoic systems of the Rocky Mountain region, USA: Denver, Colorado, Rocky Mountain Section, SEPM (Society for Sedimentary Geology), p. 415–440.

Fenneman, N.M., and Johnson, D.W., 1946, Physiographic divisions of the conterminous U.S: U.S. Geological Survey data release, https://doi.org/10.5066/P9B1S3K8.

Gloyn, R.W., Morgan, C.D., Tabet, D.E., Blackett, R.E., and Tripp, B.T., 1995, Mineral, energy, and ground-water resources of San Juan County, Utah: Utah Geological Survey Special Study 86, 44 p., https://doi.org/10.34191/SS-86.

Gregory, H.E., 1938, The San Juan country—A geographic and geologic reconnaissance of southeastern Utah: U.S. Geological Survey Professional Paper 188, 123 p.

Gregson, J.D., and Chure, D., 2000, Geology and paleontology of Dinosaur National Monument, Utah-Colorado, *in* Sprinkel, D.A., Chidsey, T.C.Jr., and Anderson, P.B., editors, Geology of Utah's Parks and Monuments: Utah Geological Association Publication 28, p. 155–188.

Hackman, R.J., 1952a, Photogeologic map of the Verdure-12 [Blanding North] quadrangle, San Juan County, Utah: U.S. Geological Survey Open-File Report 52-65, https://doi.org/10.3133/ofr5265.

Hackman, R.J., 1952b, Photogeologic map of the Verdure-13 [Blanding S] quadrangle, San Juan County, Utah: U.S. Geological Survey Open-File Report 52–65, https://doi.org/10.3133/ofr5265.

Haynes, D.D., Vogel, J.D., and Wyant, D.G., 1972, Geology, structure, and uranium deposits of the Cortez 1° x 2° quadrangle, Colorado and Utah: U.S. Geological Survey Miscellaneous Investigations Series Map I–629, scale 1:250,000, https://doi.org/10.3133/I629.

Hintze, L., and Kowallis, B.J., 2021, Geologic history of Utah—A field guide to Utah's rocks: Brigham Young University Department of Geology, 266 p.

Huff, L.C., and Lesure, F.G., 1965, Geology and uranium deposits of Montezuma Canyon area, San Juan County, Utah: U.S. Geological Survey Bulletin 1190, 102 p, https://doi.org/10.3133/B1190.

Hunt, G.J., Lawton, T.F., and Kirkland, J.I., 2011, Detrital zircon U-Pb geochronological provenance of lower cretaceous strata, foreland basin, Utah, *in* Sprinkel, D.A., Yonkee, W.A., and Chidsey, T.C., Jr., editors, Sevier thrust belt—Northern and central Utah and adjacent areas: Utah Geological Association Publication 40, p. 193-211.

Jepson, G., Carrapa, B., Reeher, L.J., DeCelles, P.G., Afonso, W.D., Howlett, C.J., Caylor, E.A., Sherpa, T.Z.L., Wang, J.W., and Constenius, K.N., 2025, Regional exhumation of the Laramide province: Geological Society of America Bulletin, https://doi.org/10.1130/B37625.1.

Kirby, S., 2008, Geologic and hydrologic characterization of the Dakota-Burro Canyon aquifer near Blanding, San Juan County, Utah: Utah Geological Survey Special Study 123, 57 p., https://doi.org/10.34191/SS-123.

Kirkland, J., DeBlieux, D., Hunt-Foster, R., Foster, J., Trujillo, K., and Finzel, E., 2020, The Morrison Formation and its bounding strata on the western side of the Blanding basin, San Juan County, Utah: Geology of the Intermountain West, v. 7, p. 137–195, https://doi.org/10.31711/giw.v7.pp137-195.

Kirkland, J., Suarez, M., Suarez, C., and Hunt-Foster, R., 2016, The Lower Cretaceous in east-central Utah—The Cedar Mountain Formation and its bounding strata: Geology of the Intermountain West, v. 3, p. 101–228, https://doi.org/10.31711/giw.v3.pp101-228.

Kjemperud, A.V., Schomacker, E.R., and Cross, T.A., 2008, Architecture and stratigraphy of alluvial deposits, Morrison Formation (Upper Jurassic), Utah: American Association of Petroleum Geologists Bulletin, v. 92, no. 8, p. 1055–1076, https://doi.org/10.1306/03250807115.

Larrieu, K., 2022, RiverREM: Online, https://github.com/OpenTopography/RiverREM, accessed January 2023.

Lucas, S.G., 2014, Lithostratigraphy of the Jurassic San Rafael Group from Bluff to the Abajo Mountains, southeastern Utah—Stratigraphic relationships of the Bluff Sandstone: Volumina Jurassica, v. 12, no. 2, p. 55–68, https://doi.org/Doi:10.5604/17313708.

Miller, C.F., 1955, Photogeologic map of the Elk Ridge-16 [Black Mesa Butte] quadrangle, San Juan County, Utah: U.S. Geological Survey Miscellaneous Geologic Investigations Map63, scale 1:24,000, https://doi.org/10.3133/i63.

Miller, C.F., 1956, Photogeologic map of Elk Ridge-9 [Mancos Jim Butte] quadrangle, San Juan County, Utah: U.S. Geological Survey Miscellaneous Geologic Investigations Map 127, scale 1:24,000, https://doi.org/10.3133/i127.

Miller, R.D., 2015, The Lower Cretaceous Cedar Mountain Formation of eastern Utah—A comparison with the coeval Burro Canyon Formation, including new measured sections on the Uncompahgre Uplift: Logan, Utah State University, M.S. thesis, 95 p.

Montgomery, S.B., 1980, Geology of Recapture Creek dam and reservoir site: Utah Division of Water Resources unpublished report, 56 p.

Murray, K.E., Reiners, P.W., Thomson, S.N., Robert, X., and Whipple, K.X., 2019, The thermochronologic record of erosion and magmatism in the Canyonlands region of the Colorado Plateau: American Journal of Science, v. 319, no. 5, p. 339–380, https://doi.org/10.2475/05.2019.01.

Pipiringos, G.N., and O'Sullivan, R.B., 1978, Principal unconformities in Triassic and Jurassic rocks, Western Interior United States—A preliminary survey: U.S. Geological Survey Report 1035-A, 38 p.

Rasmussen, C., Mundil, R., Irmis, R.B., Geisler, D., Gehrels, G.E., Olsen, P.E., Kent, D.V., Lepre, C., Kinney, S.T., Geissman, J.W., and Parker, W.G., 2021, U-Pb zircon geochronology and depositional age models for the Upper Triassic Chinle Formation (Petrified Forest National Park, Arizona, USA)—Implications for Late Triassic paleoecological and paleoenvironmental change: Geological Society of America Bulletin, v. 133, no. 3–4, p. 539–558, https://doi.org/10.1130/B35485.1.

Repenning, C.A., Cooley, M.E., and Akers, J.P., 1969, Stratigraphy of the Chinle and Moenkopi Formations, Navajo And Hopi Indian Reservations Arizona, New Mexico, and Utah: U.S. Geological Survey Professional Paper 521-B, 40 p., https://doi.org/10.3133/pp521B.

Slattery, J.S., Cobban, W.A., Mckinney, K.C., Harries, P.J., and Sandness, A.L., 2013, Early Cretaceous to Paleocene paleogeography of the Western Interior Seaway—The interaction of eustasy and tectonism: Wyoming Geological Association Guidebook 68, https://doi.org/10.13140/RG.2.1.4439.8801.

Slaughter, S.L., and Hubert, I.J., 2014, Geomorphic mapping of the Chehalis River floodplain, Cosmopolis to Pe Ell, Grays Harbor, Thurston, and Lewis counties, Washington: Washington Division of Geology and Earth Resources Information Circular 118, 63 p.

Sprinkel, D.A., 2024, Geologic map of the Duchesne 30′ x 60′ quadrangle, Duchesne and Wasatch Counties, Utah: Utah Geological Survey Map 300, scale 1:62,500, https://doi.org/10.34191/M-300DM.

Stokes, W.L., and Pheonix, D.A., 1948, Geology of the Egnar-Gypsum Valley area, San Miguel and Montrose Counties, Colorado: U.S. Geological Survey Oil and Gas Investigation Map 93, https://doi.org/10.3133/om93.

Surpless, K.D., Alford, R.W., Barnes, C., Yoshinobu, A., and Weis, N.E., 2023, Late Jurassic paleogeography of the U.S. Cordillera from detrital zircon age and hafnium analysis of the Galice Formation, Klamath Mountains, Oregon and California, USA: Geological Society of America Bulletin v. 136, no. 3–4, p. 1488–1510, https://doi.org/10.1130/B36810.1.

Tschudy, R.H., Tschudy, B.D., and Craig, L.C., 1984, Palynological evaluation of Cedar Mountain and Burro Canyon formations, Colorado Plateau: U.S. Geological Survey Professional Paper 1281, 24 p., https://doi.org/10.3133/pp1281.

Turner, C.E., and Peterson, F., 2004, Reconstruction of the Upper Jurassic Morrison Formation extinct ecosystem—a synthesis: Sedimentary Geology, v. 167, no. 3–4, p. 309–355, https://doi.org/10.1016/j.sedgeo.2004.01.009.

U.S. Geological Survey, 2018, 3D Elevation Program 1-Meter Resolution Digital Elevation Model: Online, https://apps.nationalmap.gov/downloader/, accessed December 2022.

U.S. Geological Survey, 2024, 3D Elevation Program 1-Meter Resolution Digital Elevation Model: Online, https://apps.nationalmap.gov/downloader/, accessed December 2022.

Utah Division of Oil, Gas and Mining, 2025, Division of Oil, Gas and Mining Well Formation Tops: Online, https://oilgas.ogm.utah.gov/oilgasweb/live-data-search/lds-well/well-formation-tops-lu.xhtml, accessed October 2024.

Walker, J.D., and Geissman, J.W., 2022, Geologic time scale V. 6.0: Geological Society of America, https://www.geosociety.org/GSA/gsa/timescale/home.aspx.

Willis, G.C. and Higgs, K.A., 2024, Geology of Bears Ears National Monument, Utah, *in* Sprinkel, D.A., Chidsey, T.C., Jr., Anderson, P.B., and Willis, G.C., editors, Geology of Utah's Parks and Monuments: Utah Geological Association Publication 28 (fourth edition), p. 149-200.

Witkind, I.J., 1964, Geology of the Abajo Mountains area, San Juan County, Utah: U.S. Geological Survey Professional Paper 453, 171 p., https://doi.org/10.3133/pp453.

Yonkee, W.A., and Weil, A.B., 2015, Tectonic evolution of the Sevier and Laramide belts within the North American Cordillera orogenic system: Earth-Science Reviews, v. 150, p. 531–593, https://doi.org/10.1016/j.earscirev.2015.08.001.

Young, R.G., 1960, Dakota Group of Colorado Plateau: American Association of Petroleum Geologists Bulletin, v. 44, no. 9, p. 1582–1590, https://doi.org/10.1306/BC74370D-16BE-11D7-8645000102C1865D.

Zamanian, K., Pustovoytov, K., and Kuzyakov, Y., 2016, Pedogenic carbonates—Forms and formation processes: Earth-Science Reviews, v. 157, p. 1–17, https://doi.org/10.1016/j.earscirev.2016.03.003.